ACS Chemical Neuroscience

Research Article

pubs.acs.org/chemneuro

Structural Analysis of Dopamine- and Amphetamine-Induced Depolarization Currents in the Human Dopamine Transporter

Qiong-Yao Tang,[†,§] Renata Kolanos,[‡] Louis J De Felice,*[,†] and Richard A Glennon*[,‡]

[†]Department of Physiology and Biophysics, Virginia Commonwealth University School of Medicine, Richmond, Virginia 23298, United States

[§]Jiangsu Province Key Laboratory of Anesthesiology, Xuzhou Medical College, Xuzhou 221004, People's Republic of China

[‡]Department of Medicinal Chemistry, Virginia Commonwealth University School of Pharmacy, Richmond, Virginia 23298, United States

ABSTRACT: Amphetamine (AMPH) induces depolarizing currents through the human dopamine transporter (hDAT). Recently we discovered that the *S*(+) enantiomer of AMPH induces a current through hDAT that persists long after its removal from the external milieu. The persistent current is less prominent for *R*(−)AMPH and essentially absent for dopamine (DA)-induced currents. Related agents such as methamphetamine also exhibit persistent currents, which are present in both frog oocyte and mammalian HEK expression systems. Here, we study hDAT-expressing *Xenopus laevis* oocytes voltage-clamped and exposed from outside to DA, *S*(+)AMPH, *R*(−)AMPH, and related synthesized compounds, including stereoisomers. The goal of the study was to determine how structural transitioning from dopamine to amphetamine influences hDAT potency and action. At saturating concentrations, *S*(+)AMPH or *R*(−)AMPH induce a sharply rising depolarizing current from −60 mV that is comparable in amplitude to DA-induced currents. The magnitude and duration of the currents and the presence or absence of persistent currents depend on the concentration, duration of exposure, and chemical structure and enantiomeric versions of the agents.

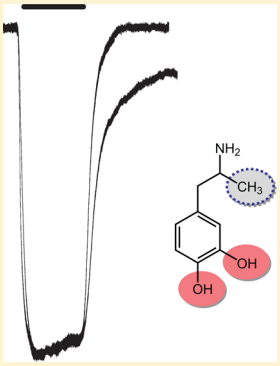

KEYWORDS: *Human dopamine transporter, dopamine, amphetamine, deconstruction, electrophysiology, Xenopus oocyte expression*

One molecular target for amphetamine (AMPH) and amphetamine-like drugs, including methamphetamine (METH) and certain synthetic cathinones, is the human dopamine transporter, hDAT,[1] which is critical to dopaminergic signaling, reward pathways, DAT internalization, and substance abuse and addiction.

Cocaine and AMPH (**1**) critically modulate the dopaminergic system in the human brain by increasing extracellular dopamine (DA; **2**) through reduced uptake.[1l,2] Cocaine blocks uptake via hDAT, whereas AMPH competes with DA uptake through the transporter. Amphetamine also releases DA into the synaptic cleft by mechanisms that are only partially understood.[1i] Two models have been proposed for AMPH-induced DA release. One is reverse transport, which relies on AMPH-induced vesicular release of DA into the presynaptic terminal;[1c,m,3] the other is docked vesicle fusion that releases DA directly into the synaptic cleft.[1d,h,4] Both mechanisms implicate depolarization of the presynaptic membrane where hDAT is located. In a previously published work, we described this depolarization current in detail alongside a new phenomenon in which *S*(+)AMPH maintains hDAT in an open state long after *S*(+)AMPH is removed from the external milieu.[1j] This open state results in a so-called "persistent current" through hDAT that would also depolarize the presynaptic membrane and, we posited, open Ca^{2+} channels and stimulate fusion of docked vesicles and DA release.[1h,4b]

Amphetamine (**1**) and DA (**2**) are structurally similar (Figure 1), and both compounds generate depolarizing currents through hDAT; if a cell contains hDAT, then AMPH or DA will induce an inward current that would depolarize the cell from its resting potential. Inspection of the two structures would seem to indicate that the hydroxyl groups of DA (absent in AMPH) or the α-methyl group of AMPH (absent in DA) make little contribution to their common initial depolarizing action. Alternatively, the absence of one of these moieties might balance the presence of the other. In addition to the initial depolarizing event, we have noted a persistent current for *S*(+)AMPH but not *R*(−)AMPH or DA. The structural moieties that are indifferent to, or responsible for, these functional characteristics are unknown. To examine this, we prepared and studied a series of agents that systematically transition from the DA (**2**) structure to the AMPH (**1**) structure.

RESULTS

Agents examined in this investigation are shown in Figure 1. The measured parameters are EC_{50} values, defined by fitting the Hill equation to the normalized DA-induced current through hDAT as a function of compound concentration. EC_{50} values

Received: November 6, 2014
Accepted: January 16, 2015
Published: January 16, 2015

DOI: 10.1021/cn500282f
ACS Chem. Neurosci. 2015, 6, 551−558

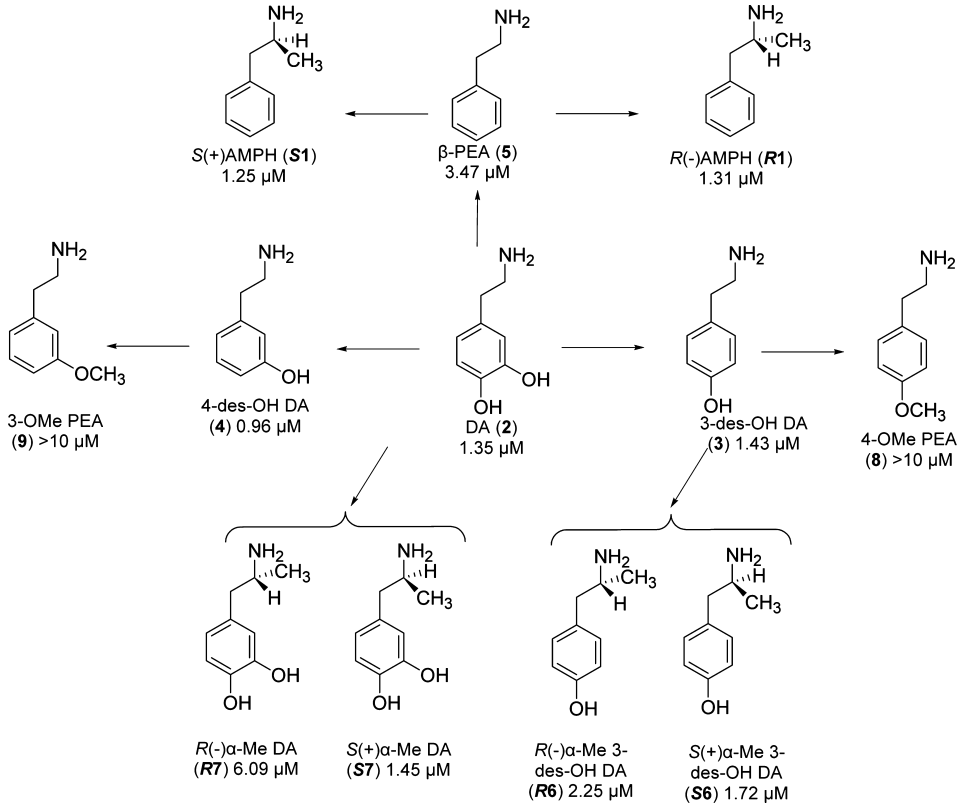

Figure 1. Agents examined with their EC_{50} values. Each arrow represents a single structural modification.

are included for each compound in Figure 1 and Table 1. The "peak" current is the initial current after adding the drug. The

Table 1. Summary of Agents Tested, Their EC_{50} Values, Hill Coefficient Values, and Ability To Generate a Persistent Current at 10 μM and −60 mV

compounds	EC_{50} (μM)	Hill coefficients	persistent current
DA (**2**)	1.35 ± 0.06	1.32 ± 0.07	no
R(−)AMPH (*R*I)	1.31 ± 0.22	0.82 ± 0.09	no
S(+)AMPH (*S*1)	1.25 ± 0.14	1.33 ± 0.17	yes
3-des-OH DA (**3**)	1.43 ± 0.17	0.91 ± 0.08	no
4-des-OH DA (**4**)	0.96 ± 0.08	1.07 ± 0.09	no
β-PEA (**5**)	3.47 ± 0.18	1.06 ± 0.16	yes
R(−)*α*-Me 3-des-OH DA (*R*6)	2.25 ± 0.21	0.98 ± 0.08	no
R(−)*α*-Me DA (*R*7)	6.09 ± 0.52	0.55 ± 0.06	no
S(+)*α*-Me 3-des-OH DA (*S*6)	1.72 ± 0.38	0.49 ± 0.05	no
S(+)*α*-Me DA (*S*7)	1.45 ± 0.50	0.71 ± 0.11	no

persistent current amplitude, I_p, is measured in two ways: (1) the time constant for recovery, T_{50}, after removal of the test compound and (2) the current remaining after drug removal and relative to the peak current. Since 10 μM DA reaches the maximum (saturating) activation of current, we normalized test currents to the DA peak current to compare cells with different hDAT expression levels. Likewise, we normalized T_{50} to the DA recovery time.

When oocytes expressing hDAT are held at −60 mV (i.e., near the resting potential of excitable cells), DA (EC_{50} = 1.35 μM) induces a current that depolarizes the cell (Figure 2). A similar depolarizing current occurs when the oocyte is exposed to *R*(−)AMPH (EC_{50} = 1.31 μM). However, exposing the oocyte to *S*(+)AMPH (EC_{50} = 1.25 μM) generates not only the initial depolarizing current but also an additional phenomenon: namely, after removal of *S*(+)AMPH from the external milieu, a cocaine-sensitive current persists (Figure 2). Cocaine also blocks the DA- and *R*(−)AMPH-induced initial currents and in all cases results in an apparent outward current that is actually the obstruction of a leak through hDAT, which is present even in the absence of an hDAT stimulus. Figure 2E shows a dose response for these three compounds. Fitting these data to the Hill equation demonstrates approximately equal potency but a rank order of efficacy *S*(+)AMPH > DA > *R*(−)AMPH. Efficacies are compared relative to DA at saturating concentrations.

Removing one or the other hydroxyl group from DA (i.e., **3** and **4**; EC_{50} = 1.43 and 0.96 μM, respectively) does not significantly alter the induced current profile compared with DA (Figure 3A,B, Table 1). However, removing both hydroxyl groups results in a significantly longer return to baseline after the compound is removed; this naturally occurring compound, *β*-phenylethylamine (*β*-PEA; **5**, EC_{50} = 3.47 μM; Figure 3C and Table 1), possesses significantly weaker potency for hDAT compared with DA (see Table 1). Note that at 10 μM, addition of an *α*-methyl group to *β*-PEA (**5**) such that it is converted to *S*(+)AMPH exacerbates the persistent current, whereas as adding a methyl group such that it converts *β*-PEA to *R*(−)AMPH eliminates the persistent current. Higher concentrations (100 μM), however, produce a more pronounced persistent current in *β*-PEA (see Figure 6 for two ways to measure the persistent current).

Adding one aromatic hydroxyl group to *R*(−)AMPH does not significantly change potency (EC_{50} = 2.25 and 1.72 μM for *R*6 and *S*6, respectively). On the other hand, chirality does

DOI: 10.1021/cn500282f
ACS Chem. Neurosci. 2015, 6, 551−558

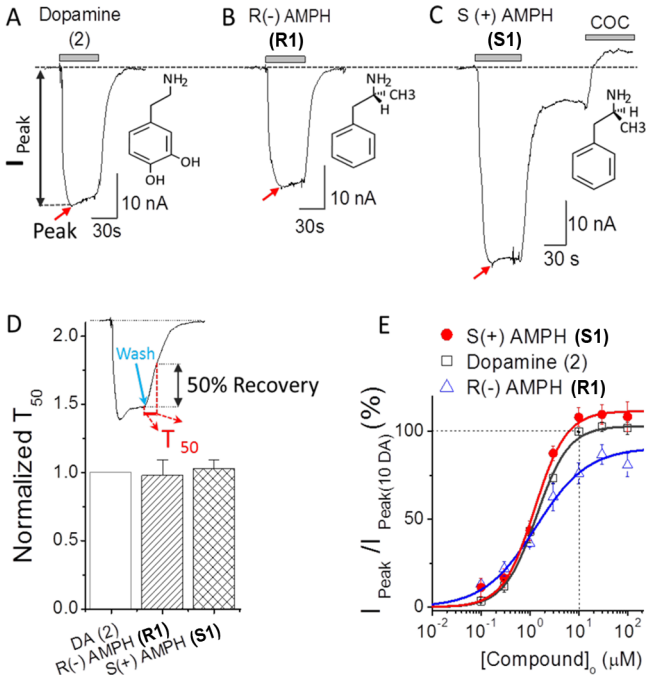

Figure 2. Dopamine (DA) and amphetamine (AMPH) induced currents. (A) Current induced by 10 μM DA at −60 mV. The inset shows the DA structure. Current returns to the original baseline upon DA removal. (B) Similar to panel A but for *R*(−)AMPH (***R1***). (C) Similar to panel A but for *S*(+)AMPH (***S1***). Note that *S*(+)AMPH induced a prominent persistent current as previously reported.[1j] The initial peak current and the persistent current are blocked by a cocaine analogue, 10 μM RTI-55, to a value positive to the baseline, suggesting the presence of an endogenous inward leak current through hDAT. (D) The recovery time, T_{50}, represents 50% return to steady current after the external test compound is removed, as indicated by the blue arrow in the inset (D). If the return time is significantly longer than it is for DA, we refer to the current as "persistent" (Figure 3). By this measure, *R*(−) AMPH is not persistent. For *S*(+)AMPH, measurement of T_{50} before the "shelf" is not significantly different from *R*(−)AMPH; on the other hand, *S*(+)AMPH appears to put the transporter in a "locked" open state (shelf) after removal, also referred to as a persistent current. β-PEA exhibits a similar locked open state at higher concentrations (Figure 6). (E) Dose−response curves for DA (open squares), *R*(−)AMPH (blue triangles) and *S*(+)AMPH (red filled circles) at −60 mV. The points at each concentration were obtained by normalizing to the 10 μM DA response in the same cell (see Methods). Solid lines are fits to the Hill equation with Hill coefficients and EC_{50} for DA of n = 1.32 ± 0.07 and EC_{50} = 1.35 ± 0.06 μM, for *R*(−)AMPH of n = 0.82 ± 0.09 and EC_{50} = 1.31 ± 0.22 μM, and for *S*(+)AMPH of n = 1.33 ± 0.17 and EC_{50} =1.25 ± 0.14 μM. The "peak" current (I_{peak}) was measured from the baseline (dotted) to the peak, indicated by red arrows. Data points represent n = 3−7 and error bars are the standard error of mean. Red arrows indicate peak depolarization upon addition of the compounds.

influence efficacy (compare Figures 4A and 5A). Adding both OH groups had little effect on the *S*-isomer (i.e., *S*7; EC_{50} = 1.45 μM) but resulted in reduced potency (*R*7; EC_{50} = 6.09 μM) and increased efficacy for the *R*-isomer compared with DA (Figures 4B and 5B and Table 1). Although the effects on potency and efficacy are slight, adding both hydroxyl groups to the aryl ring of *S*(+)AMPH completely eliminated the persistent current seen with *S*(+)AMPH (Figure 2). The O-methyl counterparts of **3** and **4** (i.e., **8** and **9**, respectively) produced similar but comparatively small depolarizing currents at a concentration of 10 μM.

The question arises whether the persistent current depends on concentration of the challenge compound. Figure 6 shows that agents with no persistent current at 10 μM induced significantly slower recoveries at 100 μM compared with DA at 100 μM. Except for 3-des-OH DA (**3**) and *R*(−)AMPH, all compounds that were tested showed slow recovery after removal of the compound. For β-PEA (**5**) note the pronounced persistent current at 100 μM compared with 10 μM (Figure 3). The efficacies of all agents at the higher concentration are, however, lower than *S*(+)AMPH.

Table 1 shows that the persistent current after removal of the compound only occurs for *S*(+)AMPH (*S*1) and β-PEA (**5**) at low concentration (10 μM), with the common feature of no hydroxyl groups on the aryl ring. The persistent current is uncorrelated with the presence or absence of the methyl group or the EC_{50} value of the test compound, although as noted above the methyl group can reduce or exacerbate the persistent current depending on its *R* or *S* configuration, respectively.

DISCUSSION

The investigation began with a deconstruction of DA to determine initially whether one or both hydroxyl groups or which of the hydroxyl groups are required for its depolarizing action. Removal of the 3-hydroxyl group of DA (**2**) affords 3-des-OH DA (**3**), whereas removal of the 4-hydroxyl group affords 4-des-OH DA (**4**). Both agents had comparable potency similar to DA. β-PEA (**5**) represents DA devoid of both hydroxyl groups, and its potency is only slightly less than DA. Evidently, neither of the hydroxyl groups of DA is required for its depolarizing action. We emphasize, however, that it is the *absence* of hydroxyl groups that correlates with the persistent current; for example, 10 μM β-PEA has a longer recovery time after removal compared with DA. This comparatively "lazy" return to baseline of β-PEA is a weak "persistence" alongside the gross flattening that occurs for β-PEA at 100 μM, reminiscent of *S*(+)AMPH. Indeed, β-PEA is the only compound other than *S*(+)AMPH with significant persistence at all concentrations. Previous evidence indicates that *S*(+)AMPH interacts with the internal face of hDAT,[1j] which would require that *S*(+)AMPH remains inside long after it is removed outside. Internal *S*(+)AMPH may lock hDAT in an open configuration, whereas the weaker form of persistence measured as T_{50} (e.g., β-PEA) may represent the internal off-rate of the compound.

Because of the relative insensitivity of DAT to the presence or absence of the hydroxyl groups of DA, it was of interest to determine whether a minor structural alteration would also be tolerated. In other words, is the transporter insensitive to aryl substitution? The O-methyl ethers of **3** and **4**, the methoxyphenylethylamines 4-OMe PEA and 3-OMe PEA (**8** and **9**, respectively), produced comparatively small depolarizing currents at a concentration of 10 μM (data not shown). It would appear, then, that a substituent at the 3- and 4-position of phenylethylamines regulates the action and potency at DAT, but that the presence of hydroxyl groups *per se* is not a requirement for the depolarization.

β-PEA (**5**) is the structural backbone of both DA (**2**) and AMPH (**1**). AMPH, the α-methyl counterpart of β-PEA, exists as a pair of optical isomers, and both were examined. The potency of *S*(+)AMPH was similar to that of its *R*(−) enantiomer and comparable to that of DA. Here too, it is shown that the hydroxyl groups are not required for the initial depolarizing action or potency. Stereochemistry played no role.

DOI: 10.1021/cn500282f
ACS Chem. Neurosci. 2015, 6, 551−558

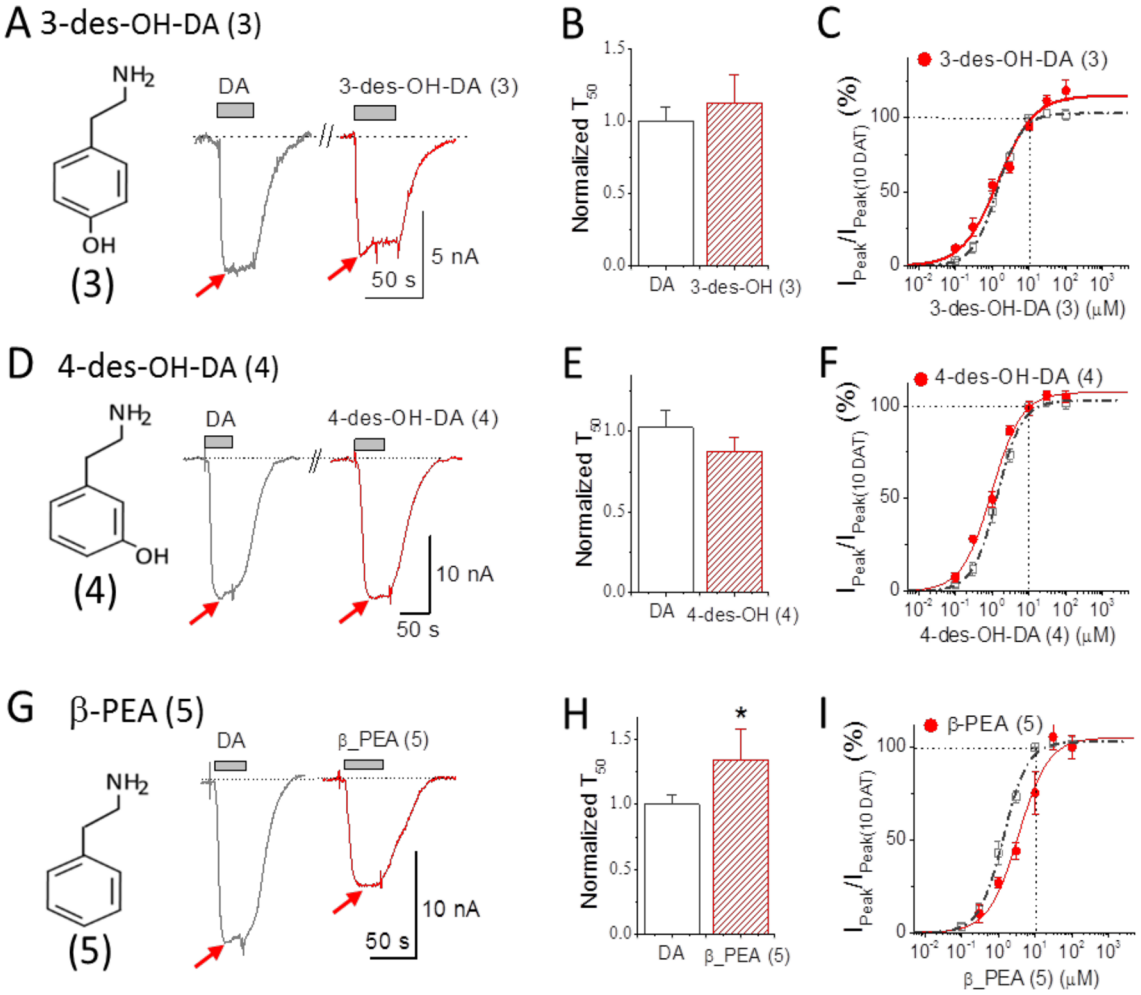

Figure 3. Depolarizing currents for deconstructed DA analogs. (A) Depolarizing action of 10 μM 3-des-OH DA (**3**) (red) compared with 10 μM DA (**2**) (black): 10 μM 3-des-OH DA is less potent than 10 μM DA and had no pronounced persistent current. The inset shows the structure of 3-des-OH DA. (B) Bars represent normalized recovery time constants at −60 mV upon removal of 10 μM DA or $R(-)\alpha$-Me 3-des-OH DA (mean ± SE, n = 4−5). (C) Dose−response curve for 3-des-OH DA (red) at −60 mV normalized to 10 μM DA in the same cell. Solid line fits the Hill equation: for 3-des-OH DA, n = 0.91 ± 0.08 and EC_{50} = 1.45 ± 0.18 μM. Panels D−F show the results of the same measurements for 4-des-OH DA (**4**) (red) compared with 10 μM DA (black): 10 μM 4-des-OH DA has similar potency to 10 μM DA and no pronounced persistent current. The inset in the left shows the structure of 4-des-OH DA. Hill equation parameters for 4-des-OH DA are n = 1.07 ± 0.09 and EC_{50} = 0.96 ± 0.08 μM. Panels G−I show the results of the same measurements for β-PEA (**5**) (red) compared with 10 μM DA (black): 10 μM β-PEA showed roughly half the potency of 10 μM DA. The recovery time upon removal of β-PEA compared with DA was significantly slowed ($P < 0.01$). Hill equation parameters for β-PEA are n = 1.06 ± 0.17 and EC_{50} = 3.47 ± 0.56 μM, which is 3 times the EC_{50} for DA. Note that T_{50} values in panels B, E, and H represent the time constant required to reach 50% recovery upon removal of the compound. For comparison, the dose−response curve for DA in Figure 1D is also shown in dashed line in panels C, F, and I. Arrows indicate peak depolarization upon addition of the compounds.

The α-methyl counterpart of DA, α-methyldopamine (α-Me DA), also exists as a pair of optical isomers: *S*7 and *R*7. The $S(+)$-isomer *S*7 is as potent as DA. The $R(-)$ enantiomer *R*7 was several-fold less potent. Introduction of an α-methyl group to 3-des-OH DA (**3**) affords α-methyl-3-des-OH DA (**6**). Both isomers were examined; the $S(+)$isomer was approximately as potent as its $R(-)$ enantiomer. Again the hydroxyl groups make a minimal contribution to the initial depolarizing potency, and stereochemistry plays, at best, a minor role.

It may appear as if the hydroxyl groups are simply "tolerated" or accommodated. However, a slight structural change (converting 4-des-OH DA and 3-des-OH DA to their corresponding O-methyl ethers, 3-OMe PEA and 4-OMe PEA, respectively; EC_{50} >10 μM) indicates that these regions are sensitive to structural alteration. Hence, whereas the presence of the individual hydroxyl groups does not contribute to the potency, the transporter is sensitive to the larger methoxy substituents.

Existing proposals for AMPH-induced increase in extracellular DA are facilitated exchange,[1h] DA efflux via channel mode or reverse transport through DAT,[1c] synaptic vesicle depletion into the presynaptic cytosol,[1m,2,5] and vesicular fusion and release of DA into the synaptic cleft via AMPH-induced currents through DAT that effect excitability and Ca^{2+} influx at the presynaptic terminal.[1d,h,4b] These models in particular depend on membrane depolarization, and understanding the chemical nature of substrate-induced depolarization is of primary interest. Not only does $S(+)$AMPH induce an initial depolarizing current similar to DA, but in our model, hDAT transports $S(+)$AMPH into the cell where it holds hDAT in an open state long after $S(+)$AMPH is removed externally. This persistently open state is therefore use-dependent with both

DOI: 10.1021/cn500282f
ACS Chem. Neurosci. 2015, 6, 551−558

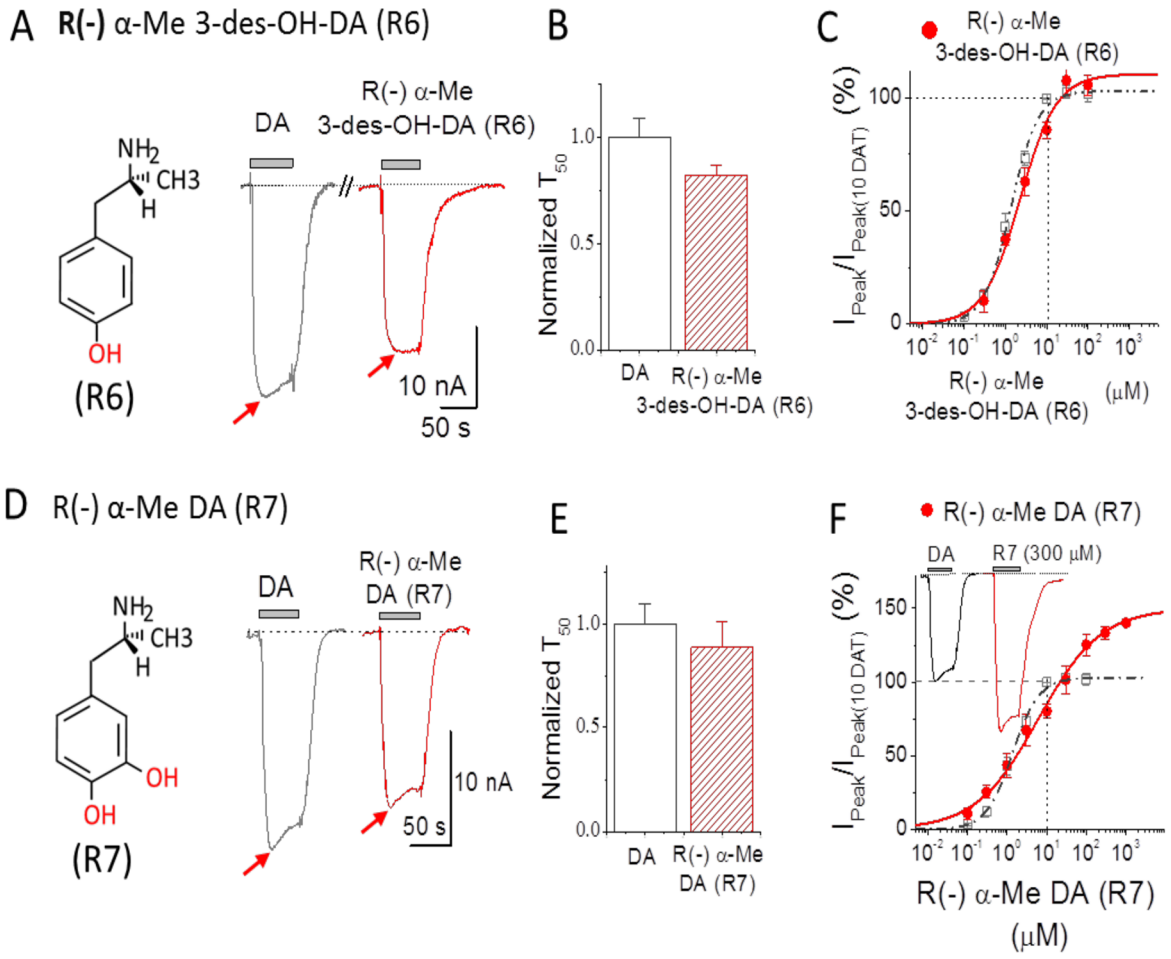

Figure 4. Depolarizing currents for *R*(−)AMPH derivatives: *R*(−)α-Me 3-des-OH DA (***R6***) and *R*(−)α-Me DA (*R7*). (A) *R*(−)α-Me 3-des-OH DA (***R6***, 10 μM) (red) compared with 10 μM DA (gray). The inset shows the structure of *R*(−)α-Me 3-des-OH DA where one hydroxyl group (red) at position 4 was added in *R*(−)AMPH. Note that *S*(−)α-Me 3-des-OH DA (***R6***) showed less potency than 10 μM DA and current returned to baseline upon removal. (B) Recovery time constants at −60 mV upon removal of 10 μM DA or *R*(−) α-Me 3-des-OH DA; rates were normalized to the equivalent experiment of 10 μM DA response in the same cell. Data points represent mean ± SE, $n = 5$. (C) Dose−response for *R*(−)α-Me 3-des-OH DA (red filled circles) at −60 mV. The points at each concentration were obtained by normalizing to the response of 10 μM DA in the same cell. Solid line is fit to the Hill equation with $n = 0.98 \pm 0.08$ and $EC_{50} = 2.25 \pm 0.20$ μM for *R*(−)α-Me 3-des-OH DA. (D) *R*(−)α-Me DA (*R7*, 10 μM) (red) compared with 10 μM DA (gray). The inset shows the structure of *R*(−)α-Me DA for which two hydroxyl groups (red) were added to *R*(−)AMPH. *R*(−)α-Me DA showed less potency than 10 μM DA and current returned to baseline after removal. (E) Recover time constants after removal of 10 μM DA or *R*(−)α- Me DA are not significantly different. Data points represent mean ± SE, $n = 4–7$. (F) Dose−response for *R*(−)α-Me DA (red filled circles) at −60 mV. The points at each concentration were normalized to 10 μM DA in the same cell. Solid line is a fit to the Hill equation with $n = 0.55 \pm 0.06$ and $EC_{50} = 6.09 \pm 0.52$ μM for *R*(−)α-Me DA, $n = 4–7$. Note that T_{50} values in panels B and E represent the time constant required to reach 50% of the recovery upon removal of the compound. For comparison, the dose−response curve from DA in Figure 1D is also shown in dashed line in panels C and F. Arrows indicate peak depolarization upon addition of the compounds.

acute and long-term effects. Furthermore, after DAT is exposed to *S*(+)AMPH, subsequent exposure to DA also results in a persistent current that indicates DAT dysfunction.[1j] DAT associated depolarization and the persistent current in particular may play a role in the known effects of AMPH on excitability in dopaminergic neurons.[1a]

The combined results suggest (a) that hydroxyl groups are not a major contributor to the initial depolarization action or potency that occurs on application of the test compounds to hDAT, (b) that stereochemistry has a minimal effect on potency but a major influence on the presence or absence of the persistent current, and (c) that the α-methyl group can affect the persistent current as it affects stereoisomers. The balance between the hydroxyl and α-methyl groups is exemplified by β-PEA, which lacks both features: β-PEA retains the initial depolarizing action, is about half as potent as DA or AMPH, and has a weak persistent current that increases with concentration.

METHODS

Chemistry. 2-(4-Hydroxyphenyl)-1-aminoethane hydrochloride (**3**) was synthesized in our laboratory as previously reported.[6] 2-(3-Hydroxyphenyl)-1-aminoethane (**4**) and 2-phenyl-1-aminoethane (or β-phenylethylamine; **5**) were purchased from AstaTech Inc. (Bristol, PA) and Sigma-Aldrich (Saint Louis, MO), respectively, as their hydrochloride salts. Isomers of 1-(4-hydroxyphenyl)-2-aminopropane hydrochloride (***S6*** and ***R6***) were prepared as reported previously.[7] Isomers of 1-(3,4-dihydroxyphenyl)-2-aminopropane hydrobromide (*S7* and *R7*) were synthesized according to the procedure described for the *R* enantiomer.[8] Melting points and optical rotations for the last two isomers have been previously reported for hydrochloride salts[9a] but not for hydrobromide salts. 2-(4-Methoxyphenyl)-1-aminoethane (**8**) and 2-(3-methoxyphenyl)-1-aminoethane (**9**) were prepared as

DOI: 10.1021/cn500282f
ACS Chem. Neurosci. 2015, 6, 551−558

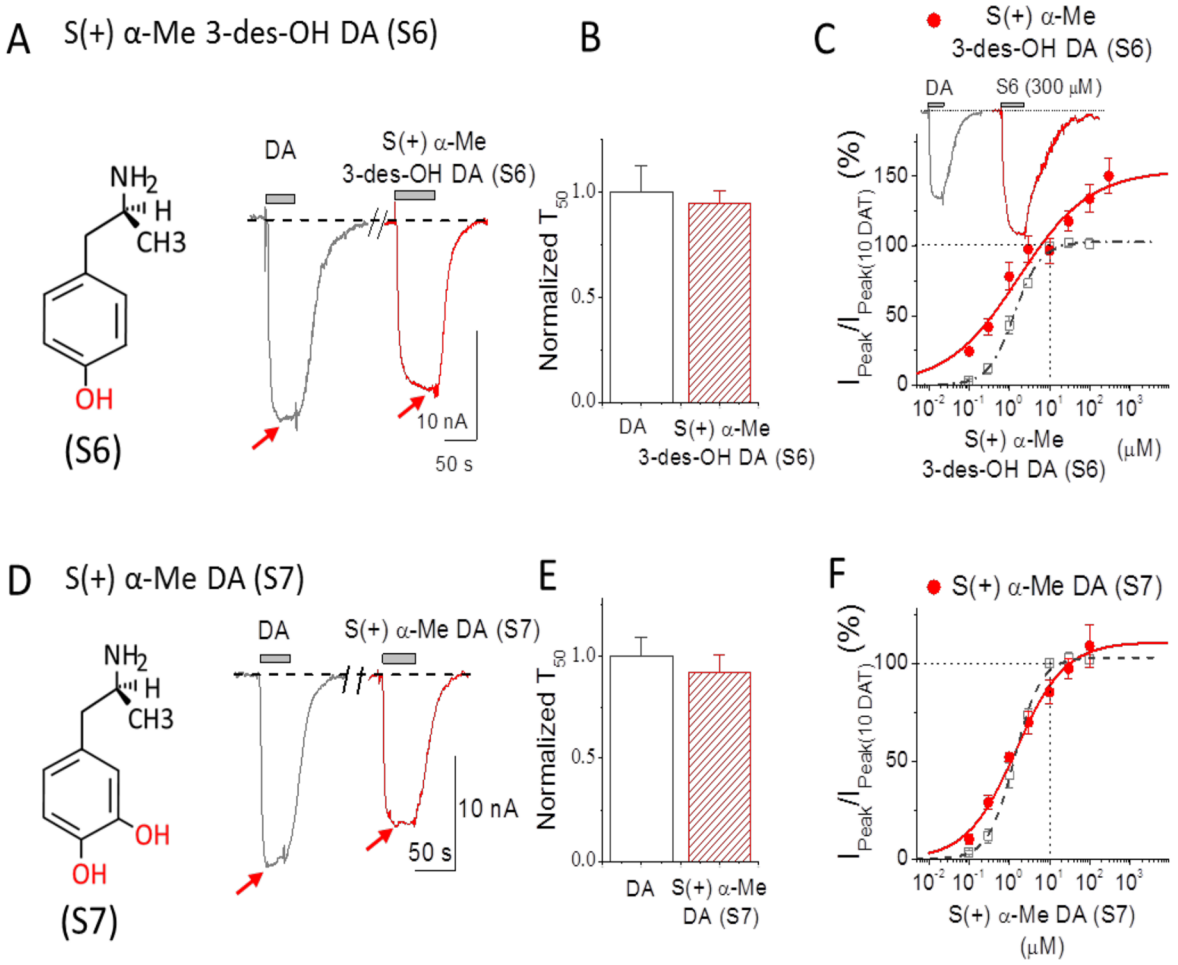

Figure 5. Depolarizing currents for the *S*(+)AMPH derivatives: *S*(+)α-Me 3-des-OH DA (*S*6) and *S*(+)α-Me DA (*S*7). (A) *S*(+)α-Me 3-des-OH DA (10 μM, red) compared with 10 μM DA (gray). The inset shows the structure of *S*(+)α-Me 3-des-OH DA with one hydroxyl group (red) added to *S*(+)AMPH at the 4-position. *S*(+)α-Me 3-des-OH DA showed similar potency compared with DA, and the current returned to baseline upon its removal. (B) Recovery time constants at −60 mV show no significant differences; rates were normalized to the equivalent experiment of 10 μM DA response in the same cell. Data points represent mean ± SE, n = 4−5. (C) Dose−response for *S*(+)α-Me 3-des-OH DA (red) at −60 mV. Points were normalized to DA response at 10 μM DA in the same cell. Solid line is fit to the Hill equation with n = 0.49 ± 0.05 and EC_{50} = 1.72 ± 0.38 μM for *S*(+)α-Me 3-des-OH DA, n = 3−6. (D) *S*(+) α-Me DA (*S*7, 10 μM, red) compared with 10 μM DA (gray). The inset on the left shows the structure of *S*(+)α-Me DA with two hydroxyl groups (red) added in *S*(+)AMPH at positions of 3 and 4. *R*(−) α-Me DA (10 μM) showed significant less potency than 10 μM DA, but current returned to baseline after removal. (E) Recovery rates at −60 mV after removing 10 μM DA or *S*(+)α-Me DA; rates were normalized to the response of 10 μM DA in the same cell. Data points represent mean ± SE, n = 5−6. (F) Dose−response for *S*(+)α-Me DA (red) normalized to 10 μM DA in the same cell. Hill equation fit gave n = 0.71 ± 0.11 and EC_{50} = 1.45 ± 0.50 μM for *S*(+)α-Me DA, n = 4−6. Note that T_{50} values in panels B and E represent the time constant required to reach 50% of the recovery upon removal of the compound. For comparison, the dose−response for DA in Figure 1D is also shown in dashed lines in panels C and F. Arrows indicate peak depolarization upon addition of the compounds.

their hydrochloride salts as previously reported.[6] Melting points were measured in glass capillary tubes (Thomas-Hoover melting point apparatus) and are uncorrected. Optical rotations were measured using a Jasco DIP-1000 polarimeter. All compounds were characterized by ^{1}H NMR, and spectra showed the expected chemical shifts. The purity of *S*7 and *R*7 (>95%) was established by elemental analysis (Atlantic Microlabs; Norcross, GA); values were within 0.4% of theory.

S(+)-1-(4-Hydroxyphenyl)-2-aminopropane Hydrochloride (S6). Mp 169−172 °C (no literature mp reported), $[\alpha]_D^{25}$ +24.7°, *c* 2.03, H_2O.

R(−)-1-(4-Hydroxyphenyl)-2-aminopropane Hydrochloride (R6). Mp 168−171 °C, (lit.[7] mp 160 °C, dec.), $[\alpha]_D^{25}$ −24.6°, *c* 2.01, H_2O (lit.[9b] $[\alpha]_D^{25}$ −26°, *c* 2.01, H_2O).

S(+)-1-(3,4-Dihydroxyphenyl)-2-aminopropane Hydrobromide (S7). Mp 164−166 °C, $[\alpha]_D^{25}$ +21.3°, *c* 2, H_2O, Anal. Calcd for $C_9H_{13}NO_2$·HBr: C, 43.57; H, 5.69; N, 5.65. Found: C, 43.56; H, 5.78; N, 5.58.

R(−)-1-(3,4-Dihydroxyphenyl)-2-aminopropane Hydrobromide (R7). Mp 163−165 °C, $[\alpha]_D^{25}$ −23.5°, *c* 2, H_2O, Anal. Calcd for $C_9H_{13}NO_2$·HBr: C, 43.57; H, 5.69; N, 5.65. Found: C, 43.59; H, 5.73; N, 5.62.

Expression of the Human DAT in *Xenopus* Oocytes. *Xenopus laevis* oocytes were harvested and prepared using the standard protocols described previously.[10] hDAT cRNA was transcribed into the pOTV vector (gift of Mark Sonders, Columbia University) using mMessage Machine T7 kit (Ambion Inc., Austin, TX) and injected within 24 h of *Xenopus laevis* oocyte isolation. Each oocyte was injected with 36−42 nL of 1 mg/mL hDAT cRNA (final amount 36−42 ng) (Nanoject AutoOocyteInjector, Drummond Scientific Co., Broomall, PA) and incubated at 18 °C in OR2(+) solution as used previously.[11] Recordings were performed 8−10 days following injection.

Two-Electrode Voltage Clamp (TEVC) in Oocytes. TEVC recordings in *Xenopus laevis* oocytes were recorded by conventional two-electrode voltage clamp as described previously.[1j,11b] The standard buffer solution perfused extracellularly is (in mM): 120 NaCl, 7.5 4-(2-

DOI: 10.1021/cn500282f
ACS Chem. Neurosci. 2015, 6, 551−558

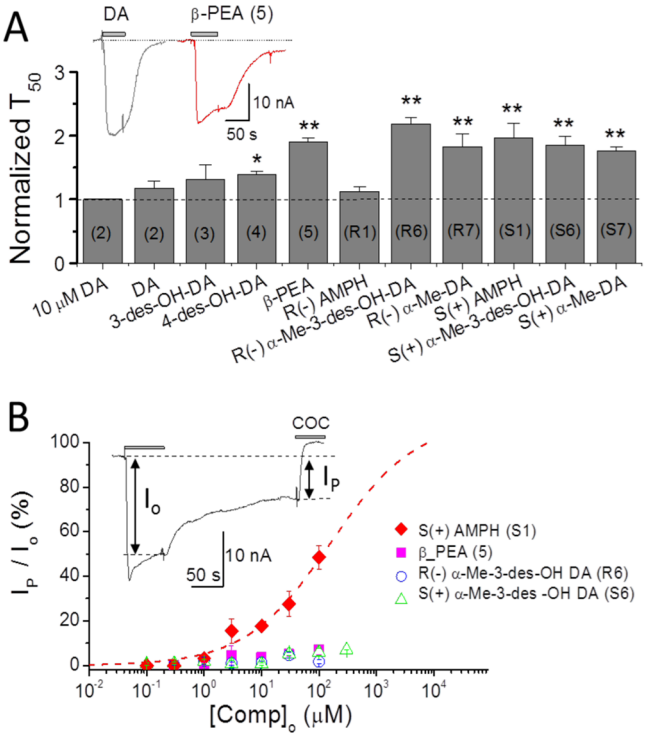

Figure 6. Depolarizing currents elicited at 100 μM concentration: persistent current defined as (A) time constant of recovery, T_{50}, or (B) current remaining after removing the compound externally (washout). (A) Time constants of recovery after removal of test compounds. All agents induce a significantly slower recovery than DA except 3-des-OH DA (**3**) and *R*(−)AMPH (*R***1**). Compounds designated with (*) or (**) and with T_{50} values greater than 1 (dotted line) are referred to as "persistent" at 100 μM; only β-PEA also passes this test at 10 μM (Figure 3). *S*(+)AMPH generates a prominent "shelf" with a flattened current, also seen at 10 μM in Figure 2, while other agents have only delayed recovery times expressed as T_{50} > 1 at this higher concentration; however, β-PEA may also show a "shelf" or "flattening", as shown in the inset. Data were recorded at −60 mV. Note that the numbers for each compound are labeled inside the column. The symbols denote **p < 0.001 and *p < 0.01. (B) The relative persistent currents of four compounds selected from panel A for slow recovery times are shown here as a function of concentration. The current I_o is the induced depolarizing current just before washout, and I_p is the current remaining after washout just before block with cocaine. Only *S*(+)AMPH (*S***1**) stands out at all concentrations; β-PEA (**5**), with relatively slow recovery and a "shelf" similar to S(+)AMPH, has a much lower persistent current than *S*(+)AMPH (*S***1**) by this definition, as do *R*(−)α-Me 3-des OH DA (*R***6**) and *S*(+)α-Me-3-des OH (*S***6**) at all concentrations.

hydroxyethyl)-1-piperazineethanesulfonic acid (HEPES), 5.4 K^+ gluconate, 1.2 Ca^{2+} gluconate, and pH 7.4 with KOH. Electrodes were filled with 3 M KCl and had resistances from 1−2 MΩ. *Xenopus* oocytes expressing hDAT were voltage-clamped to −60 mV, and the buffer was gently introduced until a stable baseline was obtained. In order to compare data from different oocytes, we perfused 10 μM DA prior the application of a particular compound and normalized all data to the first DA response (peak current at −60 mV). Dose responses for each compound were obtained by different extracellular concentrations (bath solution). For compounds that when screened showed a persistent current similar to *S*(+)AMPH, the peak and persistent currents for these compounds at each concentration were obtained from a separate oocyte injected with hDAT.

Data Analysis. Data acquisition and analysis were carried out using pClamp9 (Molecular Devices) and Origin (Microcal) software. The EC_{50} for each compound was obtained by fitting to the standard Hill equation as used previously,[10,11]

$$I/I_o(\%) = [X]_o^n/(EC_{50}^n + [X]_o^n)$$

where $I/I_o(\%)$ is the fraction of normalized current, $[X]_o$ is the drug concentration applied from the extracellular side, n is the Hill coefficient, and EC_{50} is the drug concentration required to reach half of the maximum activation.

AUTHOR INFORMATION

Corresponding Authors

*E-mail: ljdefelice@vcu.edu.
*E-mail: glennon@vcu.edu.

Funding

This work was supported by Grant NIH 1RC1DA028112-01, Grant NIH NIDA 5R01DA033930, and the Jiangsu Specially-Appointed Professor Program (Grant 53051117) to Dr. Tang.

Notes

The authors declare no competing financial interest.

ACKNOWLEDGMENTS

We thank our colleagues K. N. Cameron, Rachel Dietz, J.-M. Eltit, M. Moustafa, E. Solis Jr., T. Steele, and I. Ruchala for making valuable contributions to this work.

REFERENCES

(1) (a) Ingram, S. L., Prasad, B. M., and Amara, S. G. (2002) Dopamine transporter-mediated conductances increase excitability of midbrain dopamine neurons. *Nat. Neurosci. 5* (10), 971−978. (b) Williams, J. M., and Galli, A. (2006) The dopamine transporter: A vigilant border control for psychostimulant action. *Handb. Exp. Pharmacol.* No. 175, 215−232. (c) Kahlig, K. M., Binda, F., Khoshbouei, H., Blakely, R. D., McMahon, D. G., Javitch, J. A., and Galli, A. (2005) Amphetamine induces dopamine efflux through a dopamine transporter channel. *Proc. Natl. Acad. Sci. U. S. A. 102* (9), 3495−3500. (d) Daberkow, D. P., Brown, H. D., Bunner, K. D., Kraniotis, S. A., Doellman, M. A., Ragozzino, M. E., Garris, P. A., and Roitman, M. F. (2013) Amphetamine paradoxically augments exocytotic dopamine release and phasic dopamine signals. *J. Neurosci. 33* (2), 452−463. (e) Siciliano, C. A., Calipari, E. S., Ferris, M. J., and Jones, S. R. (2014) Biphasic mechanisms of amphetamine action at the dopamine terminal. *J. Neurosci. 34* (16), 5575−5582. (f) Siciliano, C. A., Calipari, E. S., and Jones, S. R. (2014) Amphetamine potency varies with dopamine uptake rate across striatal subregions. *J. Neurochem. 131*, 348−355. (g) Furman, C. A., Chen, R., Guptaroy, B., Zhang, M., Holz, R. W., and Gnegy, M. (2009) Dopamine and amphetamine rapidly increase dopamine transporter trafficking to the surface: live-cell imaging using total internal reflection fluorescence microscopy. *J. Neurosci. 29* (10), 3328−3336. (h) DeFelice, L. J., Glennon, R. A., and Negus, S. S. (2014) Synthetic cathinones: Chemical phylogeny, physiology, and neuropharmacology. *Life Sci. 97* (1), 20−26. (i) Goodwin, J.; Logan M.; DeFelice L.; Khoshbouei H. Methamphetamine has an exclusive target and a shared target with amphetamine to regulate dopamine transporter function. Submitted for publication, 2007. (j) Rodriguez-Menchaca, A. A., Solis, E., Jr., Cameron, K., and DeFelice, L. J. (2012) S(+)amphetamine induces a persistent leak in the human dopamine transporter: molecular stent hypothesis. *Br. J. Pharmacol. 165* (8), 2749−2757. (k) Amara, S. G., and Sonders, M. S. (1998) Neurotransmitter transporters as molecular targets for addictive drugs. *Drug Alcohol Depend. 51* (1−2), 87−96. (l) Sulzer, D. (2011) How addictive drugs disrupt presynaptic dopamine neurotransmission. *Neuron 69* (4), 628−649. (m) Sulzer, D., Chen, T. K., Lau, Y. Y., Kristensen, H., Rayport, S., and Ewing, A. (1995) Amphetamine redistributes dopamine from synaptic vesicles to the cytosol and promotes reverse transport. *J. Neurosci. 15* (5 Pt 2), 4102−4108.

DOI: 10.1021/cn500282f
ACS Chem. Neurosci. 2015, 6, 551−558

(2) Sulzer, D. (2012) How addictive drugs disrupt presynaptic dopamine neurotransmission. *Neuron 69*, 628−649.
(3) (a) Sulzer, D., Maidment, N. T., and Rayport, S. (1993) Amphetamine and other weak bases act to promote reverse transport of dopamine in ventral midbrain neurons. *J. Neurochem. 60* (2), 527−535. (b) Sulzer, D., Sonders, M. S., Poulsen, N. W., and Galli, A. (2005) Mechanisms of neurotransmitter release by amphetamines: A review. *Prog. Neurobiol. 75* (6), 406−433. (c) Kahlig, K. M., Javitch, J. A., and Galli, A. (2004) Amphetamine Regulation of Dopamine Transport. *J. Biol. Chem. 279* (10), 8966−8975.
(4) (a) De Felice, L. J., and Cameron, K. N. (2014) Comments on *A Quantitative Model of Amphetamine Action on the Serotonin Transporter*, by Sandtner et al. (2013). *Br. J. Pharmacol.*, DOI: 10.1111/bph.12767. (b) Ruchala, I., Cabra, V., Solis, E., Jr., Glennon, R. A., De Felice, L. J., and Eltit, J. M. (2014) Electrical coupling between the human serotonin transporter and voltage-gated Ca(2+) channels. *Cell Calcium 56* (1), 25−33. (c) DeFelice, L. J., and Goswami, T. (2007) Transporters as channels. *Annu. Rev. Physiol. 69*, 87−112.
(5) Sulzer, D., Maidment, N. T., and Rayport, S. (1993) Amphetamine and other weak bases act to promote reverse transport of dopamine in ventral midbrain neurons. *J. Neurochem. 60* (2), 527−535.
(6) Glennon, R. A., Liebowitz, S. M., and Anderson, L., III (1980) Serotonin receptor affinities of psychoactive phenalkylamine analogues. *J. Med. Chem. 23*, 294−299.
(7) (a) Roth G. J.; Fleck M.; Heine, N.; Kley J.; Lehmann-Lintz T.; Neubauer, H.; Nosse, B., New compounds, pharmaceutical compositions and uses thereof. WO Patent WO2012028676A1, March 8, 2012. (b) Crowell, T. A.; Evrard, D. A.; Jones, C. D.; Muehl, B. S.b; Rito, C. J.; Shuker, A. J.; Thorpe, A. J.; Thrasher, K. J. Selective fx13 adrenergic agonists. WO Patent WO9809625, March 12, 1998.
(8) Belley, L. J.; Thompson, M.; Dean, D. K.; Kotecha, N. R.; Berge, J. M.; Ward, R. W. Aryloxy and arylthiopropolamine derivatives useful as beta 3-adrenoreceptor agonists and antagonists of the beta 1 and beta 2-adrenoreceptors and pharmaceutical composition thereof. WO Patent WO9604233, February 15, 1996.
(9) (a) Pratesi, P., La Manna, A., and Grana, E. (1964) *Farmaco, Ed. Sci.* No. 19, 529−536. (b) Smith, H. E., Burrows, E. P., and Chen, F.-M. (1978) Optically active amine. 24. Circular dichroism of the para-substituted benzene chromophore. *J. Am. Chem. Soc. 100*, 3714−3720.
(10) Tang, Q. Y., Zhang, Z., Xia, J., Ren, D., and Logothetis, D. E. (2010) Phosphatidylinositol 4,5-bisphosphate activates Slo3 currents and its hydrolysis underlies the epidermal growth factor-induced current inhibition. *J. Biol. Chem. 285*, 19259−19266.
(11) (a) Tang, Q. Y., Zhang, Z., Xia, X. M., and Lingle, C. J. (2010) Block of mouse Slo1 and Slo3 K+ channels by CTX, IbTX, TEA, 4-AP and quinidine. *Channels 4*, 22−41. (b) Tang, Q. Y., Zhang, Z., Meng, X. Y., Cui, M., and Logothetis, D. E. (2014) Structural Determinants of Phosphatidylinositol 4,5-Bisphosphate (PIP2) Regulation of BK Channel Activity through the RCK1 Ca2+ Coordination Site. *J. Biol. Chem. 289*, 18860−18872.

DOI: 10.1021/cn500282f
ACS Chem. Neurosci. 2015, 6, 551−558